Molecular Dynamic Investigation of Graphene Oxide Presence and Three Experimental Distribution Methods in Reinforced Epoxy-Based Nanocomposites

Mohsen Ghiasvand [a] * , Hamid Fazeli [a], Jafar Eskandari Jam [a], Abbas Kebritchi [b]

[a] Faculty of Materials & Manufacturing Technologies, Malek Ashtar University of Technology, Tehran, Iran

[b] Department of Chemical Engineering, Imam Hossein Comprehensive University, Tehran, Iran

ARTICLE INFO

ABSTRACT

Because of the relatively high specific mechanical properties of LY556 epoxy resin, is often used as an important matrix for structural composites in high-performance applications. In the current study, an atomistic simulation based on molecular dynamics was performed to characterize the mechanical properties of LY556 epoxy (EP) nanocomposites reinforced with graphene oxide (GO) nanoparticles. The stiffness matrix and elastic properties such as Young's modulus, shear modulus, and Poisson's ratio for the pure EP and EP/GO nanocomposites were estimated using the constant-strain method. Three distribution methods including ultrasonic with a probe, mechanical mixing with an ultrasonic cleaner, and a high-shear turbo mixer with an ultrasonic cleaner were employed. The role of the distribution method on the tensile behavior of epoxy reinforced with varying percentages of GO nanoparticles (0.3 and 0.5 wt. %) was investigated. In addition, X-ray diffraction (XRD) and field emission scanning electron microscopy (FESEM) were employed to investigate the quality of GO distribution in nanocomposites. In the M3 method (the optimal method) the tensile strength of the EP/GO nanocomposite was increased about 15% (76 MPa) at 0.3 wt% and 22% (80 MPa) at 0.5 wt%. Moreover, the toughness of the EP/GO nanocomposite was improved by around 34% (1.37 J.m-3) and 50% (1.53 J.m-3) at 0.3 and 0.5 wt% respectively.

1. Introduction

In many of today's engineering applications, the combination of material properties to meet the needs of various industries is becoming more demanding. For example, aerospace industries demand materials with high strength, low density, high abrasion resistance, high UV resistance, and resistance to withstand high service temperatures. Nanocomposite materials have many of the needed characteristics/properties required by advancing industries. Moreover, in nanocomposites, unlike conventional composites, the improvement of one property does not mean a loss/degradation in other properties. In many cases, several properties can be improved simultaneously with the addition of nano reinforcements to the matrix material [1]. Due to the numerous advantageous properties

such as high stiffness, strength, and corrosion resistance exhibited by composite materials, they have swiftly secured a distinctive position in various industries. The remarkable strength-to-weight ratio of polymer matrix composites (PMCs) frequently leads to their widespread utilization [2]. Graphene nanoplatelets (GNP), carbon nanotubes (CNT), graphite, graphene oxide, and other carbon-based nanoparticles represent the new generation of materials that impart exceptional mechanical, thermal, electrical, and wear properties to composites [3, 4]. Graphene, a crucial member of carbon nanomaterials, consists of carbon atoms arranged in a two-dimensional (2D) hexagonal network. Each atom forms a strong covalent bond with three other carbon atoms, with an average bond length of 1.42 Å. [5].

The application of GNP, as a dispersed phase, is restricted by its severe hydrophobicity and gravity forces, which can contribute to the deposition of the G sheets in water-based fluids and cause these kinds of nanofluids (NF) to rarely have high stability. Stability is the most prominent feature that can limit the applications of nanofluids. So, many researchers try to improve the stability of NFs by using physical methods like ultrasonic and chemical methods [6]. GNP is the innovation of carbon-based nanoparticles that impart good thermal, mechanical, electrical, and best wear properties. It has a lower production cost than carbon nanotubes (CNT) [7, 8]. These characteristics have been reported by several researchers. Khodadadi et al. [1] investigated the possibility of improving the properties of nanocomposite using functionalization and hybridization of nanofillers in nanocomposite using molecular dynamics simulation. Takary et al. [9] performed molecular dynamics simulation to determine the interaction energy between SiO2-TiO2 nanoparticles and EP resin using MD simulation. In this research, in addition to finding the appropriate interaction of each nanoparticle individually, the performance of hybrid nanoparticles was investigated, and numerical and analytical results showed that the presence of a small amount of silica next to titanium creates a strong interaction between fillers and epoxy resin. Haghigi et al. [10] experimentally investigated the effects of filler content and the use of hybrid nanofillers on the aggregation and mechanical properties of nanocomposites such as elastic modulus, ultimate strength, and elongation to failure. In addition, two-phase and hybrid nanocomposites based on thermosetting epoxy were also simulated using multi-scale modeling techniques. The results showed that in two-phase nanocomposites, the elastic modulus and ultimate strength increase, while the

elongation to failure of the nanocomposite decreases with the weight fraction of the reinforcement.

GO is thought to be an ideal nanofiller for epoxy, the most important thermosetting resin, which is widely used in adhesives, coatings, and carbon-fiber-reinforced composites in the aerospace and aviation industries [11, 12]. Because the oxygen-containing groups of GO, i.e., the hydroxyl and epoxide groups spreading across the basal planes and the carboxyl and carbonyl groups existing at edge sites [13], facilitate the dispersion and exfoliation of GO in epoxy. They can also participate in the curing reaction of epoxy and form covalent bonds with epoxy networks. Epoxy/GO nanocomposites exhibit greatly improved fatigue characteristics and toughness [14-16]. Li et al. [17] reported effective reinforcement of GO for epoxy nanocomposites. The average tensile strength and Young's modulus were increased by approximately 11% and 24%, respectively, at a filler loading of only 0.5 wt%, without any corresponding reduction in the strain to failure. Yang et al. [18] prepared epoxy/GO nanocomposites by transferring GO from an aqueous dispersion to a DIGLYCIDYL ETHER of bisphenol-A (DGEBA)-type epoxy resin through two-phase extraction generated by lengthy vigorous stirring and heating. The compressive failure strength and toughness of the epoxy/GO nanocomposites have been greatly increased by the addition of 0.0375 wt% of GO nanosheets to the epoxy matrix. Further functionalization of GO by attaching various functional molecules or polymers provides GO with better solubility in organic solvents and augments the miscibility with hydrophobic polymers and thus improves the dispersion of GO (or rGO) and the interfacial interaction between the nanosheets and the matrices [19-24]. Such modifications have resulted in very good reinforcement of different types of polymers. For example, Wan et al. [25] grafted DGEBA to GO nanosheets and prepared epoxy nanocomposites with both unmodified GO and functionalized GO (DGEBA-f-GO) nanosheets. Improved dispersion and exfoliation of the DGEBA-f-GO nanosheets in the epoxy matrix were observed. Amino-functionalized GO was also prepared and exhibited effective reinforcement of epoxy resin because of covalent bonding between the amine groups of GO and the epoxy networks during the curing process [26, 27].

Achieving the best properties required for products relies on the homogeneous dispersion of nanofillers [25].

Sergio et al. [28] presented a method to fabricate nanocomposites from an epoxy resin reinforced with graphene oxide (GO)

nanoparticles. proposed a scalable and sustainable fabrication process, based on a solvent-free method, to achieve a high level of GO dispersion, while maintaining matrix performance. The results of the three-point bending tests show a 39% increase in the compressive elastic modulus of the nanocomposite with the addition of 0.3% by weight of GO. Yang et al. [18] reported a two-phase extraction method to prepare graphene-oxide/epoxy nanocomposites from a GO/H2O dispersion. Remarkable enhancements in compressive strength and toughness were reported, even with the incorporation of only 0.0375 wt% of GO. In another report, Wang and co-workers [11] revealed both improved thermal conductivity and low coefficients of thermal expansion (CTEs) in epoxy composites filled with 1 wt% and 5 wt% GO. The effect of GO on the epoxide curing kinetics was discussed by Bortz et al. [16] in 2011, while significant toughness and fatigue life improvements were also achieved through the addition of GO sheets. Most studies have focused on functionalized or reduced forms of GO regardless of its intrinsic behavior in epoxy composites.

The improvements in mechanical properties of nanocomposites such as flexural strength, stiffness, toughness as well and failure strain can only be achieved by a homogeneous dispersion of nanoparticles in polymeric matrices [29]. Various techniques such as shear mixing [30], mechanical stirring [29], acoustic cavitation [31], and direct incorporation/*in-situ* polymerization [32] have been utilized for the dispersion of nanoparticles in polymer matrices.

In this paper, the effects of distribution methods of graphene oxide in epoxy resin on the mechanical properties of nanocomposites, such as elastic modulus and ultimate tensile strength, are experimentally investigated. Subsequently, molecular dynamics (MD) simulation was used due to the high reliability in predicting the reaction between different materials and comparing it with the results of experimental work based on polymer-nanoparticle interaction energy. In this mode, the distribution of graphene oxide nanoparticles will be explored using various methods, including ultrasonic probe, mechanical mixing with an ultrasonic cleaner, and high shear turbo mixer with an ultrasonic cleaner. In this research, 0.3 and 0.5 wt% of graphene oxide nanoparticles are added to epoxy resin, the extracted tensile strength is compared by numerical solution, and the results are reported. In this article, the effects of three different methods of experimental distribution in nanocomposites on the mechanical properties were simultaneously investigated, and based on the results optimum method was presented.

2. Molecular Dynamics Method

Molecular dynamics is a method by which the movement of a system of N particles can be obtained by numerical calculations of Newton's equations of motion, for a specific interatomic potential, with known initial conditions and known boundary conditions. Consider a system of N atoms in volume Ω. The internal energy of this system is E=K+U, where K is the kinetic energy in the system [33].

$$K = \sum_{i=1}^{N} \frac{1}{2} m_i |\dot{x}_i(t)|^2 \tag{1}$$

and U is the potential energy of the system:

$$U = U\left(x^{3N}(t)\right) \tag{2}$$

$x^{3N}(t)$ represents the location in three dimensions of the collection of all atoms. E is a constant quantity, meaning that if the system is properly isolated, it has a constant value over time. In a molecular dynamics simulation, five elements should be considered, including boundary conditions, initial conditions, force calculation, integral and system properties calculation [33].

Two methods are used to calculate the elastic coefficients in the numerical solution the molecular dynamics method, which is the static method or constant strain, and the dynamic method [34]. In the static method, by applying small amounts of strain to the cell, the structure is deformed. At the same time, other strains are kept at zero. Then the unstable system is brought to equilibrium, and when the system reaches equilibrium, the stress corresponding to it is calculated by viral theory, and the stiffness matrix C_{ij} of the system is obtained as the derivative of stress concerning the corresponding strain [35].

$$C_{ij} = \frac{\Delta \sigma_i}{\Delta \varepsilon_j} \tag{3}$$

In this equation, σ_{ij} is calculated through the following equation.

$$\sigma = \frac{-1}{V_0} \left(\sum_{i<j} r_{ij} f_{ij}^T \right) \tag{4}$$

In the above equation, r_{ij} and f_{ij} represent the atomic distance and the corresponding interaction force between the two atoms that are in the distance of the cutoff radius, respectively. V_0 represents the total volume of the representative volumetric element.

The stiffness matrix coefficients obtained for homogeneous materials have a similar pattern to the following matrix coefficients [36]. Because of the random orientation of GOs, the material was almost isotropic, for which the

elastic stiffness matrix follows a particular pattern, as shown in Eq. (5):

$$C_{ij} = \begin{bmatrix} \lambda + 2\mu & \lambda & \lambda & 0 & 0 & 0 \\ \lambda & \lambda + 2\mu & \lambda & 0 & 0 & 0 \\ \lambda & \lambda & \lambda + 2\mu & 0 & 0 & 0 \\ 0 & 0 & 0 & \mu & 0 & 0 \\ 0 & 0 & 0 & 0 & \mu & 0 \\ 0 & 0 & 0 & 0 & 0 & \mu \end{bmatrix} \quad (5)$$

Thus, the stress-strain relations can be completely described by two Lame constants, λ and μ, calculated from the stiffness constants.

$$\lambda = \frac{1}{6}(C_{12} + C_{13} + C_{21} + C_{23} + C_{31} + C_{32}) \quad (6)$$

$$\mu = \frac{1}{3}(C_{44} + C_{55} + C_{66}) \quad (7)$$

Finally, the engineering elastic constants can be described in terms of the Lame constants, according to the following equations:

$$E = \frac{\mu(3\lambda + 2\mu)}{\lambda + \mu} \quad (8)$$

$$G = \mu \quad (9)$$

$$K = \lambda + \frac{2}{3}\mu \quad (10)$$

$$\upsilon = \frac{\lambda}{2(\mu + \lambda)} \quad (11)$$

E, K, and G represent Young's modulus, Bulk modulus, and shear modulus, respectively, and ν represents Poisson's ratio [36]. Applying the above-mentioned procedure, the mechanical properties of pure EP and EP/GO samples were calculated and averaged over all valid configurations.

The constant strain method has been used to extract mechanical properties in numerical solution.

2.1. Construction of Crosslinked DGEBA/MTHPA Models

The process of simulating molecular dynamics in modeling and optimization of nanocomposite in the Materials Studio simulation software is as follows:

The molecular structure of DGEBA is shown in Figure 1. Considering that the actual average degree of polymerization (DP), *n*, is in the range of 0.1-0.2 in experimental research[37], 0 DP is a reasonable approximation. We set the DP of DGEBA to 0 when modeling the molecular model. The model-building process is as follows:

Construct the monomer molecular models of DGEBA, MTHPA, and DGEBA-MTHPA; optimize the geometric structures of the monomer molecules under the COMPASS force field; obtain the molecular models as shown in Figure 2.

The actual reaction molar ratio of DEGBA to MTHPA is about 1:2. Accordingly, construct 10 models with 10% crosslinking density in which each model contains 40 DGEBA molecules, 90 MTHPA molecules, and 10 DGEBA-MTHPA, and 10 uncrossinked models containing 50 DGEBA molecules and 100 MTHPA molecules, respectively. The temperature was set to 600 K, and the initial density of models was 0.6 g/cm^3. After geometric structure optimization, the models with the lowest energy were selected for further simulation [38].

After the crosslinking process, the DGEBA/MTHPA models with crosslinking densities of 15%, 34%, 51%, 67%, 82%, and 96% were structurally optimized according to the energy minimum principle in the COMPASS force field. It can be concluded that the number of crosslinked bonds increases with the increasing crosslinking density, and the crosslinking reaction occurs continuously [38].

In the simulation process, after minimizing the energy of the system, to achieve a stable molecular structure for the graphene oxide/epoxy nanocomposite, the system is respectively under NVT conditions (denoting the constant number of atoms, volume, and temperature in the simulation process) and NPT (denoting the constant number of atoms, pressure, and temperature in the simulation process) is placed [35].

Geometry optimization and energy minimization were applied to the molecular structures using a smart algorithm which is a combined algorithm of the steepest descent, adopted-basis Newton-Raphson (ABNR), and quasi-Newton methods to reach the nearest local minimum with convergence tolerance of 0.0001 (kcal/mol) [39].

In this investigation, a dynamic approach is used to simulate the cross-linking process. The process includes a cyclic set of minimization, equilibration, and bonding to construct the final crosslinked structure [40]. In the equilibrium phase, the first NVT dynamics was conducted to the molecular model at a temperature of 600 K for a simulation time of 100 ps. The initial resin density was assumed to be 0.6 g/cm^3, to give a large initial spacing between the molecules. The system was subjected to 50 ps NPT dynamics simulation at a temperature of 300 K at a pressure of 1atm [40].

The stored structures undergo minor strains in the NVT process following an initial energy

minimization. The maximum amount of applied strain is 0.003, three pairs of tensile-compressive strain and three pairs of pure shear deformation are applied to the model separately. This is while other strains are considered zero and are applied in the form of a specific strain pattern. After the system reaches equilibrium, the mechanical properties are extracted by using the relations mentioned above [35].

Pure epoxy simulation is formed from the equivalent molecule of LY556 epoxy resin along with the curing agent and the molecules are randomly placed together and the polymer cell is created in MD software. As shown in Figure 3, the simulation of epoxy reinforced with graphene oxide nanoparticles with 0.3 and 0.5 wt% is created using graphene oxide molecules and polymer cells.
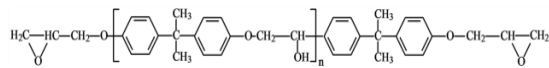

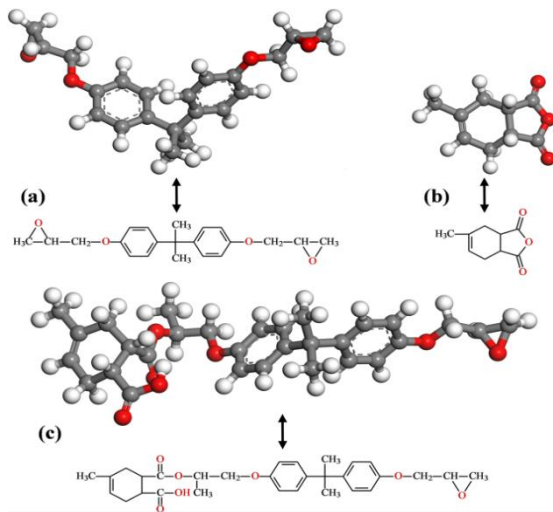**Fig. 1.** Molecular structure of DGEBA[38].

Fig. 2. Molecular models of (a) DGEBA, (b) MTHPA, (c) DGEBA-MTHPA. Gray, carbon; Red, oxygen; White, hydrogen[38].
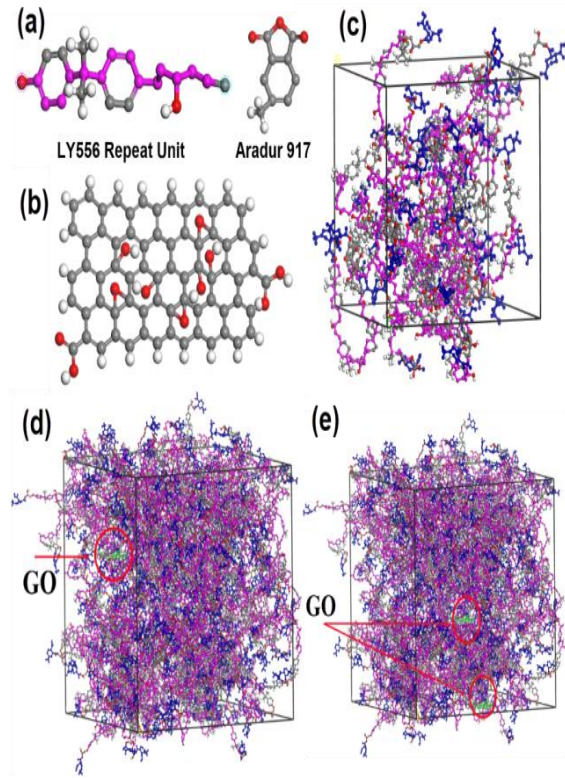

Fig. 3. Molecular structure and snapshots of created models (a) Chemical structures of LY556 with a curing agent; (b) Structure of graphene oxide molecule; (c) Cell made of pure epoxy; (d) Cell made of epoxy with 0.3 wt% graphene Oxide; (e) cell composed of epoxy with 0.5 wt% graphene oxide.

The MD simulation box details are listed in Table 1 After creating and analyzing neat epoxy models, Chain1 was selected to create nanocomposite models in Materials Studio software. This selection aimed to model nanocomposites considering the high aspect ratio and lower computational costs. In other words, nanocomposites, which comprised a 75% resin cross-linking ratio reinforced with nanofillers, were modeled using molecular dynamics [39].

Table 1. MD simulations box details.

Sample	Number of Molecules	wt (%)	Simulation Box Dimensions (Å)	Number of Chain1 resin (75% crosslinking ratio)
Epoxy	21	100	42×42×41.7	33
GO	0	0		
Epoxy	230	99.695	93.2×93.2×93.2	116
GO	1	0.305		
Epoxy	280	99.499	99.6×99.6×99.6	128
GO	2	0.501		

3. Materials and Research Method

3.1. Materials

Graphene oxide nanoparticle from FINE NANO company, produced by an Indian company (UNITED NANOTECH INNOVATIONS PVT.LTD.) in the form of powder with a thickness of 3-6 nanometers and lateral dimensions of 5-10 micrometers, 8-10 layers, density 0.42 g/cc and with a production purity of about 99% was prepared and used as reinforcing fillers in the present work. Epoxy resin equivalent to LY556, curing agent HY917, and accelerator DY070 were purchased from an Indian company named HERENBA INSTRUMENTS & ENGINEERS and used with a combination of 100, 90, and 2 weight percent. The desired resin was cured at 80°C for 4 hours and post-cured at 120°C for 4 hours to achieve the final mechanical properties of the resin. The rate of reaching the mentioned temperatures was 1.3°C/min.

3.2. Tests

In this research, three methods were used to distribute graphene oxide nanoparticles in the epoxy resin matrix and methyl ethyl ketone (MEK) solvent was used to dilute the polymer.

The first method (M1) entails the use of an ultrasonic probe. In this method, as shown in Figure 4, by dissolving graphene oxide nanoparticles in the solvent, the nanoparticles were exposed to ultrasonic probe waves for 30 minutes with a power of 50 watts for distribution. After that, epoxy resin was added to the solution and distributed for another 30 minutes with the same power in the ultrasonic probe device (Figure 7). The solvent was then extracted using an evaporator device, followed by the addition of the curing agent and accelerator. The resulting mixture was thoroughly mixed, and finally, samples were prepared for the tensile test. The casting and curing steps adhered to the ASTM D638 standard.
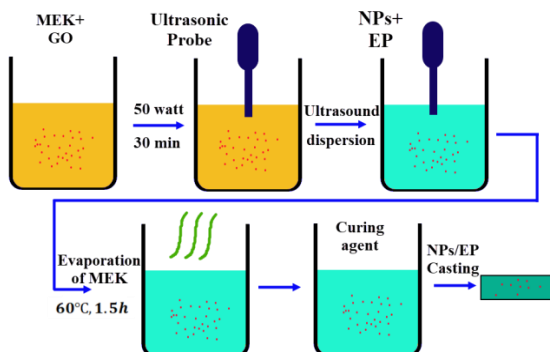
The second method (M2) involves utilizing mechanical mixing and an ultrasonic cleaner. In this method, as shown in Figure 5, by dissolving graphene oxide nanoparticles in the solvent and adding epoxy resin, distribution was done with a mechanical mixing for 30 minutes at a speed of 2000 rpm. Subsequently, an additional 30 minutes of distribution at a power of 50 watts was carried out using an ultrasonic cleaner (Figure 7). Following the mechanical mixing and ultrasonic distribution, solvent extraction was conducted using an evaporator device. Subsequently, the curing agent and accelerator were added, and the final mixing was performed. Finally, to conduct the tensile test, the fabricated samples were cast and subjected to the curing process.
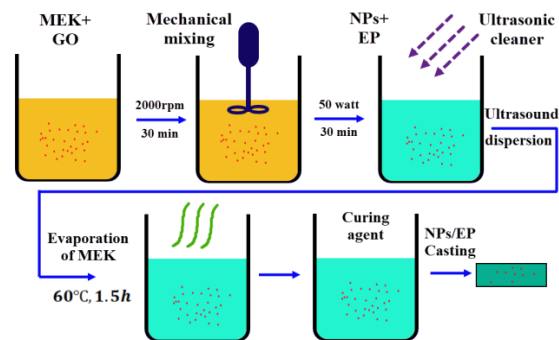

Fig. 5. A view of applying the second experimental method to distribute nanoparticles.

The third method (M3) involves the use of a high-shear turbo mixer and an ultrasonic cleaner. In this method, as shown in Figure 6, the graphene oxide nanoparticles were dissolved in the solvent, and epoxy resin was added. The distribution process included 30 minutes of mixing at a speed of 10,000 rpm using a high-shear turbo mixer. Subsequently, an additional 30 minutes of distribution at a power of 50 watts was conducted in the ultrasonic cleaner (Figure 7). After solvent extraction using the evaporator device, the curing agent and accelerator were added, followed by the final mixing step. Ultimately, to conduct the tensile test, the manufactured samples were cast and subjected to the curing process.
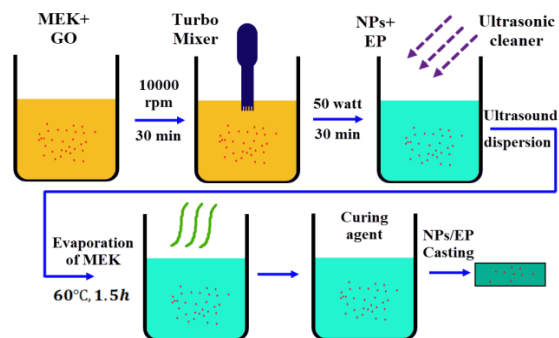

Fig. 4. A view of the application of the first experimental method for the distribution of nanoparticles.

Fig. 6. A view of applying the third experimental method for the distribution of nanoparticles.

3.3. Tensile Test Method

Tension rods were manufactured using ASTM Type IV standard with a thickness of 3.3 mm. Tensile properties were determined for all formulations under ambient conditions, utilizing ASTM D638 standards with a specimen geometry of 16.5 cm length and 3.3 mm thickness (ASTM Type IV). The tests were conducted on a mechanical testing machine (SANTAM SAF-50), with a speed rate of 1 mm/min, as illustrated in Figure 8. The tensile modulus was calculated from the initial linear part of the stress-strain curve, and at least six samples were tested for each test. Before the test, the samples were placed for 2 hours at a temperature of 23°C and a relative humidity of 50 percent.

Fig. 7. A view of (a) ultrasonic probe; (b) mechanical mixing; (c) high shear turbo mixer; (d) ultrasonic cleaner.
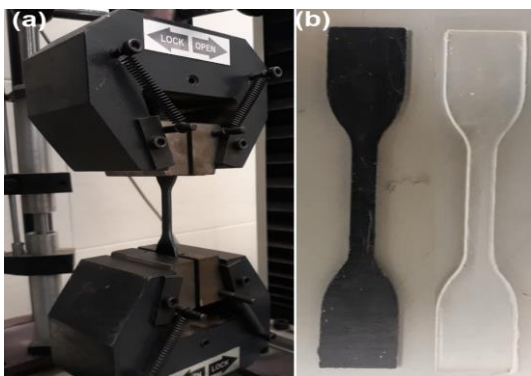

Fig. 8. A view of (a) Tensile testing machine and (b) Tensile test samples.

4. Results and Discussion

4.1. Tensile Test Results

Three molecular models were subjected to uniaxial mechanical deformations simulated by MD to predict their elastic mechanical responses. The models were deformed with 5%

uniaxial strains in tension and compression along the x, y, and z axes throughout 2 ns. Poisson contractions in transverse directions were allowed for direct calculation of Young's modulus and Poisson's ratio. The values of Young's modulus in three orthogonal directions (E_x, E_y, E_z), shear modulus (G_{xy}) in the x-y plane, and Poisson's ratios for all three samples are given in Table 2. As expected, the E_z values are much lower than the E_x and E_y values because of the van der Waals dominance in that direction and because the graphene oxide lies in the x-y plane of a line.

Table 2. Elastic properties predicted from MD simulation (modulus given in GPa)

Sample	E_x	E_y	E_z	G_{xy}	υ_{xy}	υ_{xz}	υ_{yz}
EP	1.79	1.81	1.78	0.733	0.12	0.402	0.11
EP/GO 0.3wt%	1.87	1.88	1.85	0.831	0.13	0.415	0.12
EP/GO 0.5wt%	1.93	1.94	1.91	0.982	0.15	0.432	0.13

A 3.8% increase in Young's modulus at 0.3 wt% and a 7.2% increase in Young's modulus at 0.5 wt% of graphene oxide can be seen compared to the pure resin. This behavior refers to the proper dispersion of nanoparticles in lower weight ratios. However, for higher weight ratios, the aggregation of nanoparticles prevents significant improvement of mechanical properties [41].

The mechanical properties of the experimental test samples produced were investigated in terms of tensile properties for different weight percentages of graphene oxide in epoxy resin. The results are presented in Table 3 The stress-strain curve for 0.3 wt% of graphene oxide in epoxy resin, in different states of distribution, is shown in Figure 9. Additionally, the stress-strain curve for 0.5 wt% of graphene oxide in epoxy resin, in different states of distribution, is shown in Figure 10. As depicted in Figure 11, the greatest improvement in tensile and strain properties is observed at 0.5 wt% and M3, while the highest tensile modulus is achieved at 0.5 wt% and M2.

If the amount of nanoparticles dispersed in the polymer field is appropriate, the presence of these nanoparticles reduces the movement of the polymer matrix on the common surface between the nanoparticles and the matrix, and as a result, increases the strength of the nanocomposite [42].

The continuous increase of the elastic modulus by increasing the weight percentage of nanoparticles occurs due to the proper

dispersion of nanoparticles inside the polymer matrix. The increase in the number of nanoparticles along with the proper dispersion of these particles increases the bonding and adhesion between the surface of nanoparticles and the polymer matrix, which limits the movement of polymer chains during loading. The result of this is an increase in the elastic modulus of the nanocomposite [43].

Table 3. Tensile test results of produced experimental test samples

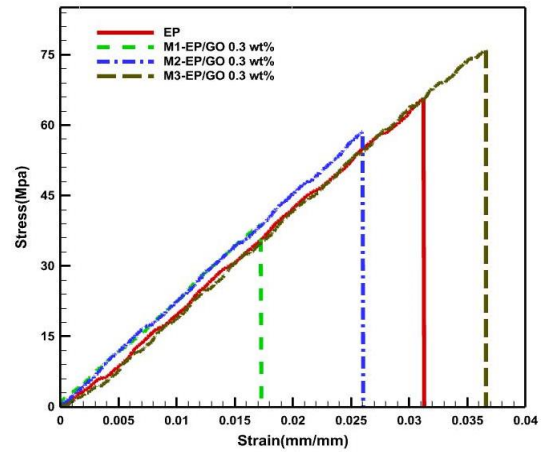| Model	Sample	Tensile Stress (MPa)	Tensile Strain (mm/mm)	Tensile Modulus (MPa)
M0	EP	65.69	0.0312	2105.5
M1	EP-GO 0.3 wt%	39.00	0.017	2294.1
	EP-GO 0.5 wt%	41.34	0.018	2296.7
M2	EP-GO 0.3 wt%	58.48	0.026	2249.2
	EP-GO 0.5 wt%	61.98	0.027	2295.5
M3	EP-GO 0.3 wt%	76.03	0.036	2111.9
	EP-GO 0.5 wt%	80.59	0.038	2120.8

Fig. 9. Axial stress-strain curves for 0.3 wt% of nanoparticles in epoxy matrix in different distribution methods.
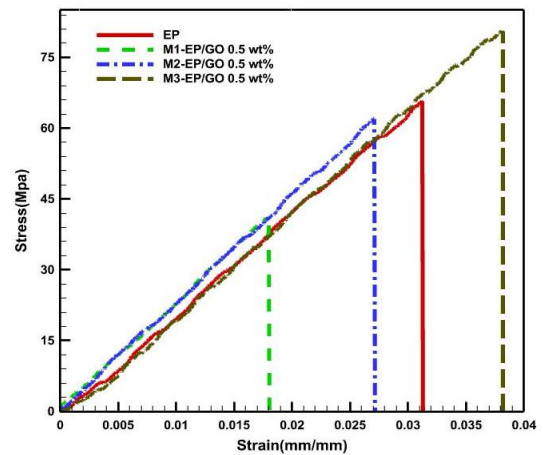

Fig. 10. Axial stress-strain curves for 0.5 wt% of nanoparticles in epoxy matrix in different distribution methods.
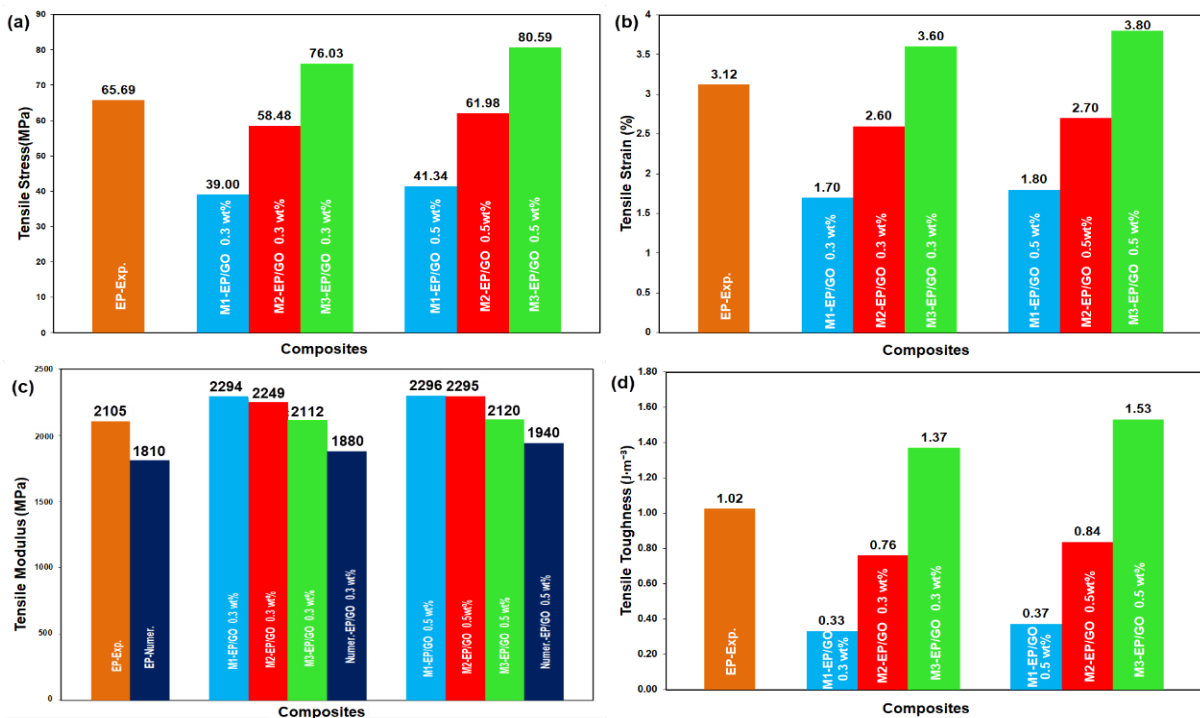

Fig. 11. A view for changes of (a) Tensile strength; (b) Tensile strain; (c) Tensile modulus; (d) Tensile toughness, depending on the type of composite

Table 2 shows the results of the elastic modulus of pure resin epoxy and nanocomposites, which were determined based on different multi-scale modeling approaches in this research. The experimental results are also listed in Table 3 for comparison. It should be noted that the percentage of improvements observed in the experimental measurements should be compared with the predicted properties. Therefore, the presented properties cannot be directly compared because the experimentally determined modulus of pure resin is lower than that predicted by multiscale models. For this reason, it was tried to make a comparison after normalization of the results which are presented in Figure 12. The difference between the experimental and predicted modulus for the pure resin and nanocomposites can be due to impurities, defects, and uncertainty in the exact chemical formula and cross-linking ratio of the resin [10].

In M3, which obtained the best properties, a 0.96% decrease (2111.9 MPa) in Young's modulus at 0.3 wt% and a 1.76% increase (2120.8 MPa) in Young's modulus at 0.5 wt% of graphene oxide compared to pure resin can be seen. The tensile strength of EP/GO nanocomposite increased by 15.7% (76.03 MPa) at 0.3 wt% and 22.7% (80.59 MPa) at 0.5 wt% compared to pure epoxy.

The mechanical properties, including strength, strain, modulus, and tensile toughness, of neat epoxy and nanocomposites with GO content in different methods are presented in Figure 11, and the values are summarized in Table 3 The greatest improvement in tensile properties (80 MPa, approximately a 22% increase), strain (about a 20.7% increase), and toughness (1.53 J.m^{-3}, approximately a 50% increase) is observed at 0.5 wt% in M3.

The highest tensile modulus (2296 MPa, about a 9% increase) is obtained at 0.5 wt% in M1 in the experimental mode. According to Table 2 in the MD method, the highest modulus is obtained at 0.5 wt% (1940 MPa, about a 7.1% increase). Figs. 12 and 13 depict a graph of normalized elastic modulus and normalized toughness, respectively. Fig. 12 displays the normalized elastic modulus values obtained from experimental and molecular dynamics methods. The obtained results were compared with other research to verify the agreement of trends as Haghighi et al.[10] and Khodadadi et al.[39] which conducted experimental and molecular dynamics studies for the investigation of Young's modulus of CNT, GNP, and CNP nanoparticles in epoxy resin. In this diagram, the M3 method exhibits more tough behavior compared to the other methods, due to lower

amounts of normalized modulus as a result of a more uniform distribution of GO nanoparticles (see 4.3. Distribution Study).

Figure 13 clearly illustrates that in the M1 method, a decrease in the elastic modulus is observed at 0.5% by weight due to the accumulation and breakage of graphene oxide sheets. In comparison with the M1 and M2 methods, the distribution method M3 demonstrates better performance in epoxy hardening.
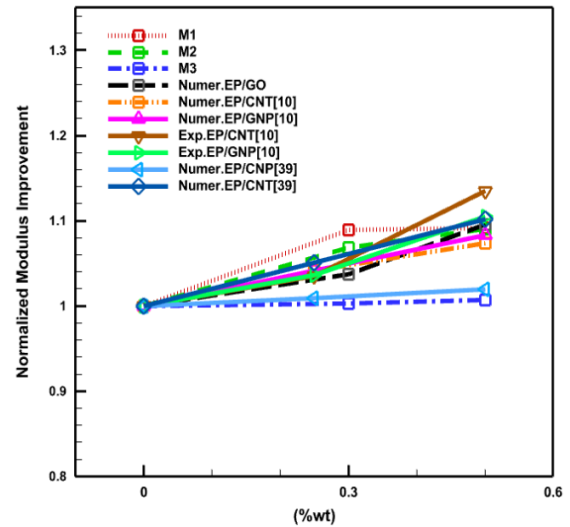

Fig. 12. A view of the normalized modulus improvement for graphene oxide content (%wt)
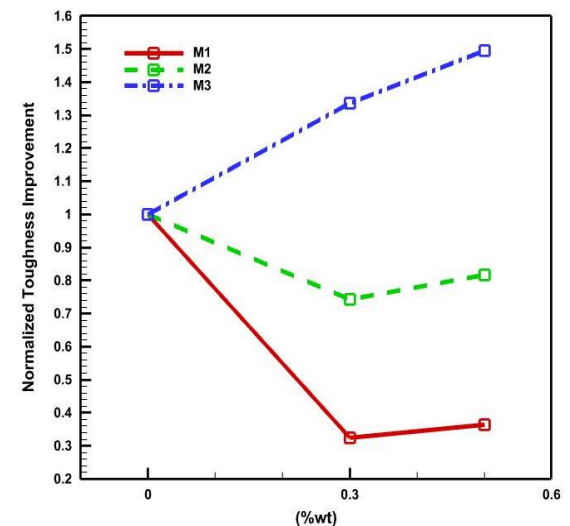

Fig. 13. A view of the normalized toughness improvement, relative to the content of graphene oxide (%wt)

4.2. Gallery Space Inspection

To comprehend the structural features of EP/GO as the base material for the multilayers produced in this research, pure graphene oxide and nanocomposites containing 0.3 and 0.5 wt%

of graphene oxide were evaluated through X-ray diffraction tests, as shown in Figures. 14 and 15.

The information obtained from the X-ray diffraction of pure graphene oxide indicates the presence of a sharp diffraction peak at the separation angle 2θ=13.39°, corresponding to the interlayer distance d=6.61 Å.

Towards the end of the diagram, peaks with lower intensity are evident at specific layer distances, as indicated in Table 4 In the X-ray diffraction analysis of nanocomposites containing 0.3 and 0.5 wt% of graphene oxide with different distribution methods, the broad diffraction peaks are observed at various separation angles and corresponding interlayer distances, as detailed in Table 4 Increasing the interlayer distance compared to the pure nanoparticle state allows the epoxy molecules to penetrate between the nanoparticle layers, which leads to a more appropriate orientation of the epoxy between these layers, and by creating a repeating regular structure, it will naturally lead to an increase in mechanical properties [44].

Certainly, the presence of a peak in the X-ray diffraction diagram of the nanocomposite containing 0.5 wt% of graphene oxide (Figure 15) suggests that the nanoparticles have formed an interlayer structure in the epoxy background without reaching a complete sheet state. Moreover, the shift in the peak position compared to pure graphene oxide indicates structural changes in the polymer network.
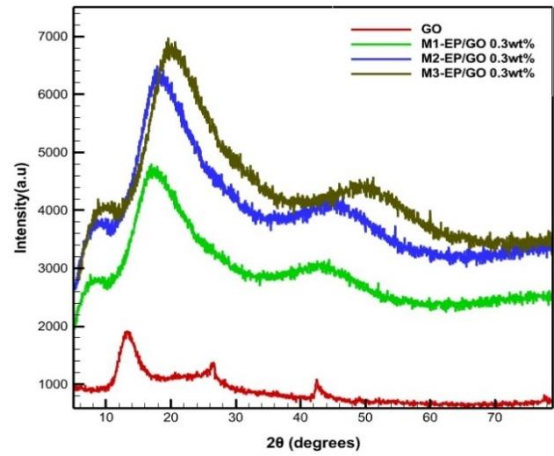

Fig. 14. X-ray diffraction curves of epoxy/graphene oxide in different distribution methods with 0.3% wt.
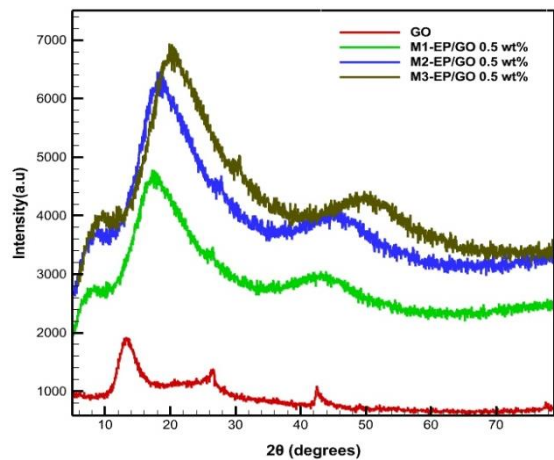

Fig. 15. X-ray diffraction curves of epoxy/graphene oxide in different distribution methods with 0.5% wt.

Table 4. Measured interplanar spacings converted to lattice constants, dispersion, and semi-quantitative analysis for all models

Model	Sample	Pos. [2θ]	Height [cts]	FWHM [2θ]	d [Å]	Rel.I. [%]
M0	GO	13.39(1)	537	2.64	6.61	100
		26.41(2)	187	0.98	3.37	34.82
		42.55(1)	181	0.56	2.12	33.67
		77.65(2)	82	0.4	1.23	15.35
M1	EP-GO 0.3% wt	7.15	741.14	11.97	12.35	99.56
		16.91	744.41	3.86	5.24	100
		43.51	295.11	9.86	2.08	39.64
	EP-GO 0.5% w	7.22	520.87	5.55	12.23	77.03
		17.39	676.21	5.12	5.09	100
		43.98	137.08	6.69	2.06	20.27
M2	EP-GO 0.3% wt	8.02	815.45	13.37	13.78	99.56
		17.89	819.05	4.45	5.96	100
		46.7	324.82	11.04	2.49	39.66
	EP-GO 0.5% wt	8.67	573.25	6.41	13.76	77.04
		18.41	744.13	5.93	5.90	100
		46.05	151.09	7.66	2.56	20.30
M3	EP-GO 0.3% wt	8.85	897.49	15.20	15.66	99.56
		19.58	901.45	5.39	7.06	100
		51.36	357.80	12.65	3.23	39.69
	EP-GO 0.5% wt	9.04	630.88	7.35	15.43	77.05
		20.00	818.84	6.82	6.79	100
		51.64	166.50	8.73	3.12	20.33

As a general rule, considering the increase in viscosity in higher percentages of nanoparticles and the possibility of clumping, the interlayer distances in high percentages of graphene oxide are typically smaller than those in samples containing lower percentages of graphene oxide. The removal of the peak related to the crystalline region of graphene oxide in the diffraction pattern of samples of different states indicates the optimal amount of nanoparticles in these nanocomposites. In general, the absence of a peak in the diffraction pattern is a sign of the complete sheeting of graphene oxide, the creation of a layer-by-layer structure in the epoxy field, and the optimal distribution of nanoparticles during the mixing process.

Due to the high aspect ratio of graphene oxide layers, the state of complete lamination leads to the creation of more contact surfaces between polymer chains and nanoparticle layers, which will naturally be associated with a significant improvement in mechanical properties [45].

4.3. Distribution Study

SEM images of the tensile test specimens' fracture surfaces were taken to show the dispersion quality of the GOs into the epoxy resin. Fig. 16 shows FESEM images of the fracture surface of nanocomposite samples in the first method (M1) with graphene oxide nanosheets reinforced with 0.3 wt% (Figure 16a) and graphene oxide nanosheets reinforced with 0.5 wt% (Figure 16b). By comparing these images, it can be concluded that the intensity of ultrasonic power with a probe increases the specific surface fracture of graphene oxide nanoparticle sheets. On the other hand, as can be seen, the background phase contains fewer graphene oxide nanosheets, which shows the distribution of nanoparticles, but the fracture of the specific surface of the sheets reduces the strength of the polymer nanocomposite. Fig. 17 shows FESEM images of nanocomposite samples in the second method (M2) with graphene oxide nanosheets reinforced with 0.3 wt% (Figure 17a) and graphene oxide nanosheets reinforced with 0.5 wt% (Figure 17b). Clumps of graphene oxide nanosheets are formed due to the unfavorable distribution of the mechanical mixing in the epoxy background, which leads to stress concentration and loss of mechanical properties. Fig. 18 shows FESEM images of nanocomposite samples in the second method (M3) with graphene oxide nanosheets reinforced with 0.3 wt% (Figure 18a) and graphene oxide nanosheets reinforced with 0.5 wt% (Figure 18b). As it is known, the high speed of the mixing has caused a favorable distribution and the ultrasonic bath has caused the absence

of lumps in the graphene oxide nanosheets and a favorable distribution in the epoxy background, which leads to an increase in mechanical properties.
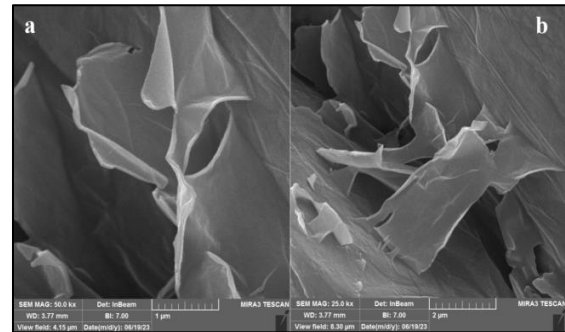

Fig. 16. A view of the fracture surface of GO nanoparticles in the first method of distribution (a) with 0.3 wt% and (b) with 0.5 wt%
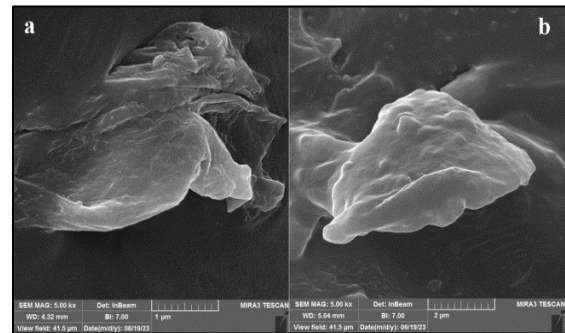

Fig. 17. A view of the agglomeration of GO nanoparticles in the second method of distribution (a) with 0.3 wt% and (b) with 0.5 wt%
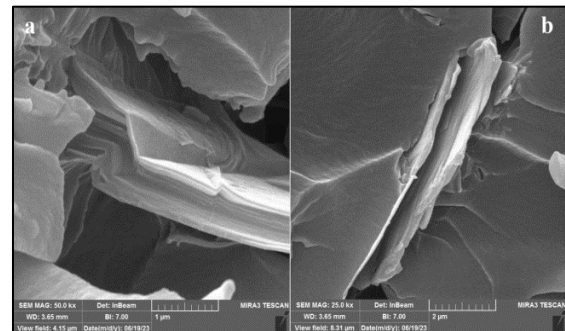

Fig. 18. A view of the optimal distribution of GO nanoparticles in the third distribution method (a) with 0.3 wt% and (b) with 0.5 wt%

5. Conclusions

Considering the high reliability in predicting the reaction between different materials and comparing it with the results of the experimental work, which is based on the polymer-nanoparticle interaction energy, molecular dynamics (MD) simulation was used, and acceptable results were obtained by comparing the experimental solution.

In this study, the tensile behavior of epoxy reinforced with different percentages of graphene oxide nanoparticles 0.3 wt% and 0.5

wt% with three distribution methods (ultrasonic with probe, mechanical mixing with an ultrasonic cleaner, and a high shear turbo mixer with an ultrasonic cleaner) was investigated. In addition, X-ray diffraction (XRD) and field emission scanning electron microscopy (FESEM) were used to investigate the quantity and distribution of graphene oxide inside the nanocomposites.

A large number of tensile specimens were fabricated and tested under uniform tensile loading until failure. The research findings can be summarized as follows:

To distribute graphene oxide nanoparticles in epoxy resin, only using the probe ultrasonic (first method), at least 30 minutes of ultrasonication at 50 watts was performed. According to the fracture surface of nanoparticle plates shown in the FESEM, the tensile strength of EP/GO nanocomposite decreased by 40.6% in 0.3 wt% and 37% in 0.5 wt% compared to pure epoxy. In the second method, mechanical mixing was used with an ultrasonic bath for at least 30 minutes at a speed of 2000 rpm and ultrasound at 50 watts to distribute graphene oxide nanoparticles in epoxy resin. According to the agglomeration of graphene oxide nanoparticles shown in the FESEM, the tensile strength of EP/GO nanocomposite decreased by 11.1% in 0.3 wt% and 5.6% in 0.5 wt% compared to pure epoxy. In the third method, a high-shear turbo mixer was used with an ultrasonic bath for at least 30 minutes at a speed of 10,000 rpm and ultrasound at 50 watts to distribute graphene oxide nanoparticles in epoxy resin. According to the optimal distribution of graphene oxide nanoparticles shown in the scanning electron microscope, the tensile strength of the EP/GO nanocomposite at 0.3 wt% is 15.7%, and at 0.5 wt% is 22.7%, and the toughness of the EP/GO nanocomposite at 0.3 wt% is 35.2%, And at 0.5 wt%, it increased by 47.9% compared to pure epoxy.

For proper distribution, without surface modification of nanoparticles, the higher the mixing speed with turbo baffled mixers, the more suitable distribution and the amount of tensile strength in different percentages of nanoparticles will be improved.

Funding Statement

Conflicts of Interest

The author declares that there is no conflict of interest regarding the publication of this article.

References

[1] Khodadadi, A., Haghighi, M., Golestanian, H. and Aghadavoudi, F., 2020. Molecular dynamics simulation of functional and hybrid epoxy-based nanocomposites. *Mechanics of Advanced Composite Structures*, 7, 233-243.

[2] Ghasemi, A. R. and Mohammadi-Fesharaki, M., 2017. Distribution of residual stresses in polymer-reinforced carbon nanotubes and laminated carbon fibers. *Mechanics of Advanced Composite Structures*, 4, 9-18.

[3] Shah, D. B., Patel, K. M., Joshi, S. J., Modi, B. A., Patel, A. I. and Pariyal, V., 2019. Thermo-mechanical characterization of carbon fiber composites with different epoxy resin systems. *Thermochimica Acta*, 676, 39-46.

[4] Sukur, E. F. and Onal, G., 2020. Graphene nanoplatelet modified basalt/epoxy multi-scale composites with improved tribological performance. *Wear*, 460, 203481.

[5] Hassanloo, H., Sadeghzadeh, S. and Ahmadi, R., 2020. A new approach to dispersing and stabilizing graphene in aqueous nanofluids of enhanced efficiency of energy systems. *Scientific Reports*, 10, 7707.

[6] Hassanloo, H., Sadeghzadeh, S. and Ahmadi, R., 2022. Reactive molecular dynamics simulation of thermo-physicochemical properties of non-covalent functionalized graphene nanofluids. *Materials Today Communications,* 32, 103869.

[7] Hawal, T. T., Patil, M. S., Kulkarni, R. M. and Nandurkar, S. N., 2020. Synergetic effect of rubber on the tensile and flexural properties of graphene based epoxy-carbon fiber hybrid nanocomposite. *Materials Today: Proceedings*, 27, 515-518.

[8] Srivatsava, M. and Sreekanth, P. R., 2020. Experimental characterization of dynamic mechanical properties of hybrid carbon-Kevlar reinforced composite with sandwich configuration. *Materials Today: Proceedings*, 27, 931-935.

[9] Takari, A., Ghasemi, A. R., Hamadanian, M., Sarafrazi, M. and Najafidoust, A., 2021. Molecular dynamics simulation and thermo-mechanical characterization for optimization of three-phase epoxy/TiO2/SiO2 nano-composites. *Polymer Testing*, 93, 106890.

[10] Haghighi, M., Golestanian, H. and Aghadavoudi, F., 2021. Determination of mechanical properties of two-phase and hybrid nanocomposites: experimental

determination and multiscale modeling. *Journal of Polymer Engineering*, 41, 356-364.

[11] Wang, Z., Shen, X., Akbari Garakani, M., Lin, X., Wu, Y., Liu, X., Sun, X. and Kim, J.-K., 2015. Graphene aerogel/epoxy composites with exceptional anisotropic structure and properties. *ACS applied materials & interfaces*, 7, 5538-5549.

[12] Hsiao, M.-C., Ma, C.-C. M., Chiang, J.-C., Ho, K.-K., Chou, T.-Y., Xie, X., Tsai, C.-H., Chang, L.-H. and Hsieh, C.-K., 2013. Thermally conductive and electrically insulating epoxy nanocomposites with thermally reduced graphene oxide–silica hybrid nanosheets. *Nanoscale*, 5, 5863-5871.

[13] Zhu, X. and Su, H., 2014. Exciton characteristics in graphene epoxide. *ACS nano*, 8, 1284-1289.

[14] Ni, Y., Chen, L., Teng, K., Shi, J., Qian, X., Xu, Z., Tian, X., Hu, C. and Ma, M., 2015. Superior mechanical properties of epoxy composites reinforced by 3D interconnected graphene skeleton. *ACS applied materials & interfaces*, 7, 11583-11591.

[15] Wang, X., Jin, J. and Song, M., 2013. An investigation of the mechanism of graphene toughening epoxy. *Carbon*, 65, 324-333.

[16] Bortz, D. R., Heras, E. G. and Martin-Gullon, I., 2012. Impressive fatigue life and fracture toughness improvements in graphene oxide/epoxy composites. *Macromolecules*, 45, 238-245.

[17] Li, Z., Young, R. J., Wang, R., Yang, F., Hao, L., Jiao, W. and Liu, W., 2013. The role of functional groups on graphene oxide in epoxy nanocomposites. *Polymer*, 54, 5821-5829.

[18] Yang, H., Shan, C., Li, F., Zhang, Q., Han, D. and Niu, L., 2009. Convenient preparation of tunably loaded chemically converted graphene oxide/epoxy resin nanocomposites from graphene oxide sheets through two-phase extraction. *Journal of Materials Chemistry*, 19, 8856-8860.

[19] Jiang, T., Kuila, T., Kim, N. H. and Lee, J. H., 2014. Effects of surface-modified silica nanoparticles attached graphene oxide using isocyanate-terminated flexible polymer chains on the mechanical properties of epoxy composites. *Journal of Materials Chemistry A*, 2, 10557-10567.

[20] Georgakilas, V., Otyepka, M., Bourlinos, A. B., Chandra, V., Kim, N., Kemp, K. C., Hobza, P., Zboril, R. and Kim, K. S., 2012. Functionalization of graphene: covalent and non-covalent approaches, derivatives and applications. *Chemical reviews,* 112, 6156-6214.

[21] Teng, C.-C., Ma, C.-C. M., Lu, C.-H., Yang, S.-Y., Lee, S.-H., Hsiao, M.-C., Yen, M.-Y., Chiou, K.-C. and Lee, T.-M., 2011. Thermal conductivity and structure of non-covalent functionalized graphene/epoxy composites. *Carbon*, 49, 5107-5116.

[22] Lu, S., Li, S., Yu, J., Yuan, Z. and Qi, B., 2013. Epoxy nanocomposites filled with thermotropic liquid crystalline epoxy grafted graphene oxide. *RSC advances*, 3, 8915-8923.

[23] Li, Z., Wang, R., Young, R. J., Deng, L., Yang, F., Hao, L., Jiao, W. and Liu, W., 2013. Control of the functionality of graphene oxide for its application in epoxy nanocomposites. *Polymer*, 54, 6437-6446.

[24] Cano, M., Khan, U., Sainsbury, T., O'neill, A., Wang, Z., Mcgovern, I. T., Maser, W. K., Benito, A. M. and Coleman, J. N., 2013. Improving the mechanical properties of graphene oxide based materials by covalent attachment of polymer chains. *Carbon*, 52, 363-371.

[25] Wan, Y.-J., Tang, L.-C., Gong, L.-X., Yan, D., Li, Y.-B., Wu, L.-B., Jiang, J.-X. and Lai, G.-Q., 2014. Grafting of epoxy chains onto graphene oxide for epoxy composites with improved mechanical and thermal properties. *Carbon*, 69, 467-480.

[26] Park, Y. T., Qian, Y., Chan, C., Suh, T., Nejhad, M. G., Macosko, C. W. and Stein, A., 2015. Epoxy toughening with low graphene loading. *Advanced Functional Materials*, 25, 575-585.

[27] Park, S. and Kim, D. S., 2014. Preparation and physical properties of an epoxy nanocomposite with amine-functionalized graphenes. *Polymer Engineering & Science,* 54, 985-991.

[28] Horta Muñoz, S., Serna Moreno, M. D. C., González-Domínguez, J. M., Morales-Rodríguez, P. A. and Vázquez, E., 2019. Experimental, numerical, and analytical study on the effect of graphene oxide in the mechanical properties of a solvent-free reinforced epoxy resin. *Polymers*, 11, 2115.

[29] Wetzel, B., Haupert, F. and Zhang, M. Q., 2003. Epoxy nanocomposites with high mechanical and tribological performance. *Composites science and technology*, 63, 2055-2067.

[30] Wetzel, B., Rosso, P., Haupert, F. and Friedrich, K., 2006. Epoxy nanocomposites–fracture and toughening mechanisms. *Engineering fracture mechanics*, 73, 2375-2398.

[31] Goyat, M., Suresh, S., Bahl, S., Halder, S. and Ghosh, P., 2015. Thermomechanical response and toughening mechanisms of a carbon nano bead reinforced epoxy composite. *Materials Chemistry and Physics*, 166, 144-152.

[32] Kang, S., Hong, S. I., Choe, C. R., Park, M., Rim, S. and Kim, J., 2001. Preparation and characterization of epoxy composites filled with functionalized nanosilica particles obtained via sol–gel process. *Polymer,* 42, 879-887.

[33] Allen, M. P. and Tildesley, D. J., 2017. Computer simulation of liquids, Oxford university press.

[34] Merhari, L., 2009. Hybrid nanocomposites for nanotechnology, Springer.

[35] Shokrieh, M., Shokrieh, Z. and Hashemianzadeh, S., 2014. Modeling of stiffness of graphene/epoxy nanocomposites with randomly distributed graphene using a combined molecular dynamics micromechanics method. *Modares Mechanical Engineering*, 13, 25-35.

[36] Farhadinia, M., Arab, B. and Jam, J., 2016. Mechanical properties of CNT-reinforced polymer Nano-composites: a molecular dynamics study. *Mechanics of Advanced Composite Structures,* 3, 113-121.

[37] Wang, X. and Wu, P., 2018. Melamine foam-supported 3D interconnected boron nitride nanosheets network encapsulated in epoxy to achieve significant thermal conductivity enhancement at an ultralow filler loading. *Chemical Engineering Journal,* 348, 723-731.

[38] Xie, Q., Liang, S., Liu, B., Fu, K., Zhan, Z., Lu, L., Yang, X., Lü, F. and Huang, Z., 2018. Structure, microparameters and properties of crosslinked DGEBA/MTHPA: A molecular dynamics simulation. *Aip Advances*, 8.

[39] Khodadadi, A., Golestanian, H. and Aghadavoudi, F., 2022. Two modified multiscale modeling approaches for determination of two-phase and hybrid nanocomposite properties. Proceedings of the Institution of Mechanical Engineers, Part C: Journal of Mechanical Engineering Science, 236, 496-510.

[40] Aghadavoudi, F., Golestanian, H. and Tadi Beni, Y., 2017. Investigating the effects of resin crosslinking ratio on mechanical properties of epoxy-based nanocomposites using molecular dynamics. *Polymer Composites*, 38, E433-E442.

[41] Sharma S, C. R., Kumar P, Kumar N., 2015. Thermo-mechanical characterization of multi-walled carbon nanotube reinforced polycar-bonate composites: A molecular dynamics ap-proach.

[42] Karippal, J. J., Narasimha Murthy, H., Rai, K., Sreejith, M. and Krishna, M., 2011. Study of mechanical properties of epoxy/glass/nanoclay hybrid composites. *Journal of Composite Materials,* 45, 1893-1899.

[43] Yasmin, A., Abot, J. L. and Daniel, I. M., 2003. Processing of clay/epoxy nanocomposites by shear mixing. *Scripta materialia*, 49, 81-86.

[44] Agubra, V. A., Owuor, P. S. and Hosur, M. V., 2013. Influence of nanoclay dispersion methods on the mechanical behavior of E-glass/epoxy nanocomposites. *Nanomaterials*, 3, 550-563.

[45] Kusmono, Z.A., Wildan, M. and Mohd Ishak, Z., 2013. Preparation and properties of clay-reinforced epoxy nanocomposites. *International Journal of Polymer Science,* 690675, 7-15.